# ENHANCEMENT OF ZnO-BASED UV PHOTODETECTORS BY INCORPORATING $Bi_2O_3$, Ag, AND Ge NANOSTRUCTURES SYNTHESIZED USING LASER ABLATION IN LIQUID

**ALHARBI ABDULLAH MARZOUQ B**

**UNIVERSITI SAINS MALAYSIA**

**2025**

# ENHANCEMENT OF ZnO-BASED UV PHOTODETECTORS BY INCORPORATING $Bi_2O_3$, Ag, AND Ge NANOSTRUCTURES SYNTHESIZED USING LASER ABLATION IN LIQUID

**by**

**ALHARBI ABDULLAH MARZOUQ B**

**Thesis submitted in fulfilment of the requirements**
**for the degree of**
**Doctor of Philosophy**

**July 2025**

## ACKNOWLEDGEMENT

In the name of Allah, Most Gracious, Most Merciful. First and foremost, I thank Almighty Allah for His mercy, guidance, and strength throughout this journey. His blessings and grace have been my source of inspiration and resilience.

I would like to express my heartfelt gratitude to my main supervisor, Assoc. Prof. Dr. Azhar Abdul Rahman, for his invaluable support, insightful guidance, and encouragement throughout my research. I am also deeply indebted to my co-supervisors, Assoc. Prof. Dr. Naser Mahmoud Ahmed and Assoc. Prof. Dr. Nurul Zahirah Noor Azman, for their thoughtful advice and expertise, which have been instrumental in shaping this work.

My deepest appreciation goes to my parents, my father, Marzouq, and my mother, Josa, whose unwavering love and support have been the foundation of all my achievements. I am also profoundly grateful to my wife, Meznah, and my children, Dimah, Azam, Marzouq, and Rimah, for their endless patience, encouragement, and understanding. Their presence has been a constant source of strength and motivation.

I would also like to thank the staff of the School of Physics, the solid-state lab, and the NOR lab at USM for their invaluable technical assistance. To my friends and colleagues, thank you for your camaraderie, support, and encouragement along the way.

May Allah reward all those who have contributed to this work in ways both great and small.

Thank You…

## TABLE OF CONTENTS

## LIST OF TABLES

**Page**

## LIST OF FIGURES

**Page**

## LIST OF SYMBOLS

| | |
|---|---|
| A/W | Ampere per Watt |
| c | Speed of light |
| CB | Conduction Band |
| D* | Detectivity |
| E | Incoming light intensity per unit area |
| Eg | Optical band gap energy |
| G | Current Gain |
| h | Planck's constant |
| hkl | Miller indices |
| Idark | Dark Current |
| Iphoto | Photocurrent |
| P | Incident light power per unit area |
| R | Responsivity (A/W) |
| S | Sensitivity (%) |
| η | Quantum efficiency |
| λ | Wavelength of incident radiation |
| Ω·m | Ohm-meter (Unit for resistivity) |

## LIST OF ABBREVIATIONS

| | |
|---|---|
| AgNPs | Silver nanoparticles |
| $Bi_2O_3$-Nsh | Bismuth oxide nanosheets |
| DC | Direct Current |
| DIW | Deionized Water |
| EDX | Energy-Dispersive X-Ray |
| EQE | External Quantum Efficiency |
| FESEM | Field Emission Scanning Electron Microscopy |
| fs | Femtosecond |
| GeNWs | Germanium nanowals |
| JCPDS | Joint Committee on Powder Diffraction Standards |
| Kiethley | Kiethley 2400 Source Meter |
| LAL | Laser Ablation in Liquid |
| LASiS | Laser Ablation Synthesis in Solution |
| LSPR | Localized Surface Plasmon Resonance |
| MAgNPs | Multi-shaped Silver Nanoparticles |
| MNW | Metallic Nanowire |
| M-S | Metal-Semiconductor |
| NEP | Noise Equivalent Power |
| NPs | Nanoparticles |
| NRs | Nanorods |
| ns | Nanosecond |
| Nsh | Nanosheets |
| NTs | Nanotubes |
| NWs | Nanowalls |

| | |
|---|---|
| PI | Polyimide |
| PLAL | Pulsed Laser Ablation in Liquid |
| PRR | Pulse Repetition Rate |
| PSi | Porous Silicon |
| PVD | Physical Vapor Deposition |
| QDs | Quantum Dots |
| RCA | Radio Corporation of America |
| RF | Radio Frequency |
| SILAR | Successive Ionic Layer Adsorption and Reaction |
| SPR | Surface Plasmon Resonance |
| UV | Ultraviolet |
| UVPD | Ultraviolet Photodetector |
| UV-Vis | Ultraviolet-Visible |
| UV-Vis-IR | Ultraviolet-Visible-Infrared |
| XPS | X-ray Photoelectron Spectroscopy |
| XRD | X-ray Diffraction |
| ZnO | Zinc Oxide |

## LIST OF APPENDICES

**PENINGKATAN PENGESAN FOTO UV BERASASKAN ZnO DENGAN KEMASUKAN NANOSTRUKTUR $Bi_2O_3$, Ag, DAN Ge YANG DISINTESIS MENGGUNAKAN ABLASI LASER DALAM CECAIR**

## ABSTRAK

Kajian ini meningkatkan kecekapan pengesan foton UV melalui sintesis dan integrasi nanopartikel menggunakan teknik ablasi laser. Penyelidikan ini meneliti kesan nanosheets bismuth oksida ($Bi_2O_3$-Nsh), nanopartikel perak (AgNPs), dan dinding nano germanium (GeNWs) pada pengesan foton UV berasaskan ZnO/Si. Dengan mengubah saiz dan bentuk nanopartikel secara tepat, kajian ini bertujuan untuk meningkatkan responsiviti, sensitiviti, dan prestasi keseluruhan pengesan. Ciri-ciri komprehensif nanopartikel yang disintesis dan integrasi mereka ke dalam seni bina pengesan telah dinilai bagi menentukan keberkesanan serta potensinya untuk aplikasi praktikal. Nanosheets $Bi_2O_3$ ($Bi_2O_3$-Nsh) telah disintesis menggunakan kaedah laser ablation in liquid (LAL). $Bi_2O_3$-Nsh ini kemudian diintegrasikan ke dalam pengesan ZnO/Si dan diuji melalui mikroskopi imbasan elektron pancaran medan (FESEM), pembelauan sinar-X (XRD), spektroskopi UV-vis, serta analisis sinar-X serakan tenaga (EDX) untuk mengkaji struktur kristal, morfologi, dan sifat optiknya. Prestasi pengesanan foton UV dinilai di bawah cahaya UV 385 nm pada voltan bias yang berbeza. Pengesan UV ZnO/ $Bi_2O_3$-Nsh/Si menunjukkan tindak balas yang kuat, dengan lengkung I-V yang meningkat ketara daripada 79 μA kepada 20 mA pada 6 V. Selain itu, peranti ini mempamerkan responsiviti tertinggi sebanyak 49.8 A/W, kecekapan kuantum 161.61, sensitiviti 25000%, keuntungan sebanyak 251, kebolehkesanan (detectivity) sebanyak $9.86 \times 10^{10}$ Jones, dan kuasa setara bunyi (NEP) sebanyak $1.01 \times 10^{-12}$ W di bawah cahaya UV 385 nm pada voltan bias 6 V.

Hasil ini menekankan potensi $Bi_2O_3$-Nsh dalam meningkatkan prestasi pengesan UV ZnO/Si. Penyelidikan ini juga mensintesis AgNPs menggunakan teknik ablasi laser yang kos efektif digabungkan dengan sputtering RF. AgNPs ini dikapsulkan dalam lapisan zink oksida pada substrat silikon untuk meningkatkan kecekapan pengesan serta mengurangkan kos. Tiga konfigurasi sampel (AgNPs/Si, AgNPs/ZnO/Si, dan ZnO/AgNPs/Si) diuji menggunakan FESEM, XRD, EDX, dan spektroskopi UV-vis. Pengesan ZnO/AgNPs/Si menunjukkan prestasi tertinggi, dengan responsiviti puncak 132 A/W, kecekapan kuantum 429.88, sensitiviti 31400%, keuntungan sebanyak 315, kebolehkesanan $18 \times 10^{10}$ Jones, dan NEP sebanyak $0.556 \times 10^{-13}$ W. Penemuan ini mengesahkan potensi AgNPs dalam meningkatkan prestasi pengesan foton UV serta keberkesanan kaedah sintesis kos efektif. Selain itu, GeNWs telah disintesis melalui ablasi laser berdenyut untuk meningkatkan pengesanan foton UV. GeNWs ini diintegrasikan ke dalam pengesan ZnO/Si dalam dua konfigurasi: ZnO/GeNWs/Si dan GeNWs/ZnO/Si. Konfigurasi ZnO/GeNWs/Si menunjukkan prestasi cemerlang dengan arus foton sekitar 12.8 mA pada 6 V, membuktikan peningkatan yang ketara dalam penyerapan cahaya UV dan pengangkutan cas pembawa. Peranti ini mempamerkan responsiviti sebanyak 31.8 A/W, kecekapan kuantum 103.43, sensitiviti 9600%, dan kebolehkesanan $4.90 \times 10^{10}$ Jones. Hasil ini menunjukkan potensi GeNWs dalam meningkatkan prestasi pengesan foton UV serta keberkesanan ablasi laser berdenyut. Penyelidikan ini berjaya mencapai objektifnya dengan menggunakan teknik ablasi laser untuk mensintesis dan mengintegrasikan $Bi_2O_3$-Nsh, AgNPs, dan GeNWs ke dalam pengesan foton UV.

**ENHANCEMENT OF ZnO-BASED UV PHOTODETECTORS BY INCORPORATING $Bi_2O_3$, Ag, AND Ge NANOSTRUCTURES SYNTHESIZED USING LASER ABLATION IN LIQUID**

## ABSTRACT

This research enhances the efficiency of UV photodetectors through the synthesis and integration of nanoparticles using laser ablation techniques. The study investigates the effects of bismuth oxide nanosheets ($Bi_2O_3$-Nsh), silver nanoparticles (AgNPs), and germanium nanowalls (GeNWs) on ZnO/Si-based UV photodetectors. By change nanoparticle size and shape, the research aims to improve responsivity, sensitivity, and overall performance. Comprehensive characterization of the synthesized nanoparticles and their integration into photodetector architectures was conducted to evaluate their effectiveness and potential for practical applications. $Bi_2O_3$ nanosheets ($Bi_2O_3$-Nsh) were synthesized using the laser ablation in liquid (LAL) method. The $Bi_2O_3$-Nsh were integrated into ZnO/Si photodetectors, and their crystalline structures, morphologies, and optical properties were characterized using X-ray diffraction (XRD), field emission scanning electron microscopy (FESEM), energy-dispersive X-ray (EDX), and UV-visible spectroscopy analysis. The UV photodetection performance was assessed under 385 nm UV light at varying bias voltages. The ZnO/$Bi_2O_3$-Nsh/Si-based UV photodetectors demonstrated a strong response, with the I-V curve showing a significant change from 79 μA to 20 mA at 6 V. Additionally, the device exhibited the highest responsivity of 49.8 A/W, quantum efficiency of 161.61, sensitivity of 25000%, gain of 251, detectivity of $9.86 \times 10^{10}$ Jones, and a noise equivalent power (NEP) of $1.01 \times 10^{-12}$ W under 385 nm UV light at a bias voltage of 6 V. These results highlight the potential of $Bi_2O_3$-Nsh in enhancing

ZnO/Si photodetectors. The research also synthesized AgNPs using a cost-effective laser ablation technique combined with RF sputtering. The AgNPs were encapsulated by zinc oxide on a silicon substrate to enhance photodetector efficiency while reducing costs. Three sample configurations (AgNPs/Si, AgNPs/ZnO/Si, and ZnO/AgNPs/Si) were characterized using FESEM, XRD, EDX, and UV-visible spectroscopy. The ZnO/AgNPs/Si photodetector exhibited the highest performance, with a peak responsivity of 132 A/W, quantum efficiency of 429.88, sensitivity of 31400%, gain of 315, detectivity of $18 \times 10^{10}$ Jones, and an NEP of $0.556 \times 10^{-13}$ W. These findings underscore the potential of AgNPs in enhancing UV photodetector performance and the feasibility of cost-effective synthesis methods. Furthermore, GeNWs were synthesized via pulsed laser ablation to improve UV photodetection. The GeNWs were integrated into ZnO/Si photodetectors in two configurations: ZnO/GeNWs/Si and GeNWs/ZnO/Si. The ZnO/GeNWs/Si configuration showed impressive performance, with a photocurrent of around 12.8 mA at 6 V, indicating significant enhancement in UV light absorption and carrier charge transport. The device exhibited a responsivity of 31.8 A/W, quantum efficiency of 103.43, sensitivity of 9600%, and detectivity of $4.90 \times 10^{10}$ Jones. These results demonstrate the potential of GeNWs to enhance UV photodetector performance and the effectiveness of pulsed laser ablation. This research successfully addresses the objectives by using laser ablation techniques to synthesize and integrate $Bi_2O_3$-Nsh, AgNPs, and GeNWs into UV photodetectors.

# CHAPTER 1

# INTRODUCTION

## 1.1 Overview

Nanoparticles (NPs) have garnered significant attention in recent years for their potential in various advanced technological applications, including ultraviolet (UV) photodetectors. UV photodetectors are critical for numerous applications such as environmental monitoring, flame detection, and biological and chemical sensing. This overview provides a concise summary of the properties and synthesis methods of bismuth oxide ($Bi_2O_3$), silver (Ag), germanium (Ge), and zinc oxide (ZnO) nanoparticles, emphasizing their relevance to UV photodetector applications.

Zinc oxide (ZnO) is a highly promising material for UV photodetectors due to its wide direct band gap (~3.37 eV), high optical transparency, and significant exciton binding energy [1, 2]. ZnO NPs can be synthesized with various morphologies, enhancing their physical properties for specific applications. The studies by Valença et al. [3] and other researchers have demonstrated the effectiveness of ZnO NPs in X-ray detectors and photocatalytic applications, highlighting their potential in UV photodetection. ZnO NPs exhibit high electron mobility and thermal stability, making them suitable for high-performance UV photodetectors. Their ability to form nanorods, nanowires, and other nanostructures further enhances their applicability, allowing for the design of devices with tailored properties for specific UV detection needs [4]. Additionally, ZnO's non-toxic and abundant nature makes it an environmentally friendly option for large-scale production and deployment in various UV photodetection applications, from consumer electronics to industrial monitoring systems.

Bismuth oxide ($Bi_2O_3$) is characterized by its high density (9.78 g/cm³), low thermal conductivity (7.97 W/mK), and significant X-ray attenuation properties due to its high atomic number. Specifically, bismuth oxide ($Bi_2O_3$) nanoparticles are advantageous in UV photodetectors due to their high mass absorption coefficient and effective optical properties in the UV-visible spectrum. Studies, such as those by Torrisi et al. and Verma et al., [5, 6] have demonstrated the efficacy of $Bi_2O_3$ NPs in imaging and radiotherapy, which can be extrapolated to UV detection applications. These properties also contribute to the enhanced sensitivity and efficiency of UV photodetectors utilizing $Bi_2O_3$ NPs, as they can absorb and convert UV light effectively, making them ideal for applications where high sensitivity to UV radiation is crucial.

Silver nanoparticles (Ag NPs) exhibit unique optical properties, high electrical conductivity, and strong interactions with specific wavelengths of light due to surface plasmon resonance (SPR). This makes Ag NPs particularly useful in UV photodetectors. The work by Alqanoo et al., [7] has shown that Ag nanowires can significantly enhance the performance of photodetectors through their plasmonic absorption properties, thereby improving sensitivity and spectral selectivity in UV detection. The conduction and valence bands of Ag NPs are proximate where electrons are freely mobile, giving rise to an SPR absorption band. This SPR effect can be tuned by altering the size and shape of the nanoparticles, enabling the design of photodetectors with specific UV sensitivity and high performance [8]. Additionally, Ag NPs are known for their antimicrobial properties, making them useful in medical and environmental monitoring applications where UV photodetection is required [9].

Germanium nanoparticles (Ge NPs) are known for their small band gap, excellent charge transport properties, and IR photoluminescence. These characteristics, combined with their low toxicity and high mechanical stability, make Ge NPs suitable for a range of optoelectronic applications, including UV photodetectors. Studies by Achour et al. and Stavarache et al. [10, 11] have demonstrated the effectiveness of Ge NPs in enhancing near-infrared (NIR) detector performance. Notably, through quantum confinement effects in nanoscale Ge, the bandgap can be widened, allowing absorption in shorter wavelengths, which broadens its potential for UV photodetector technologies. Additionally, combining Ge with materials like ZnO, which is inherently responsive to UV light, can further optimize its use in UV-visible detection, highlighting its adaptability across different photodetection applications. The small energy required to create an electron-hole pair in Ge (2.9 eV) compared to gases or scintillators, results in a high number of electron-hole pairs produced per incident photon, leading to better energy resolution and higher sensitivity in UV photodetection [12]. This makes Ge NPs particularly advantageous for applications requiring precise and high-resolution UV detection, such as in scientific research and advanced imaging technologies.

## 1.2 Overview of Laser Ablation in Liquid (LAL)

Laser ablation in liquid (LAL) is a versatile and increasingly popular method for synthesizing nanoparticles with unique properties. This technique employs a high-energy laser to ablate a target material submerged in a liquid medium, leading to the formation of nanoparticles. The size and morphology of the nanoparticles produced by LAL are highly dependent on specific parameters and preparation techniques, such as laser wavelength, pulse duration, laser fluence, and the type of liquid medium used.

These factors significantly influence the characteristics of the resulting nanoparticles [13]. Compared to other nanoparticle synthesis techniques, LAL offers several distinct advantages. One of the primary benefits is the production of stable products with minimal agglomeration, which is crucial for applications requiring consistent particle performance [14]. The simplicity of the synthesis process also makes LAL an attractive option, as it does not require complex chemical setups or extensive post-processing steps [15]. Furthermore, LAL is capable of producing monodisperse nanoparticles, meaning the particles have a uniform size distribution, which is highly desirable for various technological and biomedical applications [16].

LAL is also an eco-friendly technique, typically involving the use of water or other benign solvents, reducing the environmental impact compared to methods that rely on hazardous chemicals [17]. The reaction times for LAL are relatively short, allowing for rapid production of nanoparticles. This aspect, coupled with the cost-effectiveness of the method, makes it suitable for large-scale production [18]. Moreover, the nanoparticles produced through LAL are often of high purity, as the laser ablation process can effectively remove contaminants from the target material [19]. One of the most significant advantages of LAL is the change it offers over particle size and shape. By adjusting laser parameters such as fluence and pulse duration, researchers can finely tune the properties of the nanoparticles to meet specific requirements. This level of change is particularly beneficial for applications in electronics, medicine, and catalysis, where the performance of nanoparticles is highly dependent on their size and morphology [20].

This method involves irradiating a solid target immersed in a liquid using laser pulses, leading to the ejection and rapid cooling of material to form nanoparticles. Key studies, such as those by Lin et al. and Gondal et al., [21, 22] have successfully

synthesized $Bi_2O_3$ NPs using laser ablation for photocatalytic and optical applications. Laser ablation parameters, such as laser wavelength, pulse duration, and fluence, significantly influence the properties of the synthesized nanoparticles. For instance, Ag NPs have been synthesized using laser wavelengths of 355 nm and 532 nm, with varying laser fluences to control stability and size distribution [23]. Similarly, Mg NPs and Au-Ag NPs have been synthesized with specific laser settings to optimize their structural and optical properties [24, 25]. The laser ablation technique allows for change over nanoparticle characteristics, making it ideal for producing nanoparticles with specific properties required for high-performance UV photodetectors. This method also offers eco-friendliness, cost-effectiveness, and the ability to produce stable and high-purity nanoparticles, making it a valuable tool in the advancement of nanoparticle-based UV photodetectors.

## 1.3 Overview of Photodetectors

Photodetectors are crucial devices in various optical systems, converting light into electrical signals for applications in telecommunications, medical imaging, environmental monitoring, and scientific research. They operate based on the photoelectric effect, where incident photons generate electron-hole pairs in a material, producing a measurable current or voltage. Key performance parameters include responsivity, quantum efficiency, response time, dark current, and noise equivalent power, all of which determine the sensitivity, speed, and overall performance of the photodetector [26].

Common types of photodetectors include photodiodes, phototransistors, avalanche photodiodes, and photomultiplier tubes, each offering unique advantages for specific applications. Advances in materials science have introduced novel

materials such as silicon, germanium, and two-dimensional materials like graphene, enhancing performance through high carrier mobility and tunable bandgaps. Integration with other components, such as microelectromechanical systems (MEMS) and optical fibers, has led to multifunctional devices with improved spatial resolution and high-speed data transmission capabilities. These advancements continue to expand the applications and effectiveness of photodetectors in modern technology [27].

## 1.4 Problem Statement

The key issue addressed in this study is the compromised stability and performance of synthesized nanomaterials — specifically bismuth oxide ($Bi_2O_3$) nanosheets, silver (Ag) nanoparticles, and germanium (Ge) nanowalls — when integrated onto silicon (Si) substrates, particularly under thermal and electrical stress conditions. These challenges are critical in the development of high-performance ultraviolet (UV) photodetectors. Factors contributing to performance degradation include atomic diffusion from the nanoparticles, electromigration of electrons induced by electrical stress, and oxidation reactions triggered by changes in ambient conditions, as previously reported [28, 29]. For example, joule heating has been shown to destabilize networks of metallic nanostructures such as Ag nanowires, leading to failure of device performance [30]. Oxidative degradation further compromises the structural integrity and optical properties of $Bi_2O_3$ and Ge nanostructures [31, 32]. To address these issues, this study proposes the incorporation of a zinc oxide (ZnO) layer, aimed at enhancing the thermal and electrical stability of the $Bi_2O_3$, Ag, and Ge nanoparticles, preventing atomic diffusion, minimizing electromigration, and shielding against oxidation. Furthermore, the study investigates how nanoparticle morphology and interface engineering influence the photoelectric response, aiming to

optimize the performance and reliability of UV photodetectors based on Si substrates. This approach aims to improve the resilience and performance of metallic NPs in practical applications where stability is paramount.

## 1.5 Objectives

The objectives of this study can be summarized as follows:

i. To synthesize and characterize $Bi_2O_3$, Ag, and Ge nanoparticles with controlled size and shape using laser ablation, and to assess their individual contributions to enhancing UV photodetector efficiency on silicon substrates.

ii. To investigate the effects of ZnO layer positioning with $Bi_2O_3$, Ag, and Ge nanoparticles on the stability and performance of UV photodetectors.

iii. To comprehensively evaluate the electrical and optical performance of the fabricated UV photodetectors under different configurations, focusing on responsivity, sensitivity, stability, and detectivity.

## 1.6 Novelty of This Work

The novelty of this work lies in its innovative approach to enhancing the stability and performance of UV photodetectors through the synthesis and integration of $Bi_2O_3$, Ag, and Ge nanoparticles using a laser ablation technique, coupled with the strategic incorporation of a ZnO layer. This research addresses a critical challenge in the field: the thermal, electrical, and chemical instability of metallic and oxide nanoparticles when deposited on silicon substrates. By introducing a ZnO interlayer,

the study mitigates issues related to atomic diffusion, electromigration, and oxidation, thereby significantly improving the durability and photoelectric performance of $Bi_2O_3$, Ag, and Ge nanostructures. Furthermore, the laser ablation technique enables precise control over nanoparticle size and shape, which is crucial for optimizing their optical and electrical properties for UV detection applications. This work also systematically investigates the effect of ZnO layer positioning relative to the nanoparticles, providing new insights into enhancing radiation detection capabilities. Through comprehensive characterization, including crystal structure, surface morphology, optical absorption, and electrical behavior analysis, this research advances the understanding of material-device interactions. The outcomes of this study contribute to the development of highly efficient, stable, and scalable UV photodetectors, with promising prospects for deployment in advanced optoelectronic and sensing technologies.

## 1.7 Scope of Study

This research focuses on the development and optimization of advanced UV photodetectors through the innovative use of $Bi_2O_3$, Ag, and Ge nanoparticles. The study involves synthesizing nanoparticles via laser ablation in distilled water, ensuring high purity and changed size and shape. Effective deposition methods using drop coating techniques will be developed to achieve a uniform and stable layer of nanoparticles on silicon substrates. To enhance stability and efficiency, the research will investigate incorporating a ZnO layer, comparing its effects when positioned above or below the nanoparticles. Comprehensive characterization using techniques such as X-ray diffraction (XRD), and Field Emission Electron Scanning Microscopy (FESEM), will evaluate the key performance metrics, including photosensitivity, response times, quantum efficiency, and detectivity. The study aims to optimize these

nanomaterial-based photodetectors for practical applications in environmental monitoring, addressing challenges related to the stability and performance of metallic nanoparticles. Ultimately, the findings will contribute to the advancement of UV photodetector technology, providing valuable solutions for real-world applications.

## 1.8 Outline of Thesis

The thesis is divided into five chapters, beginning with the study's introduction, problem statement, objectives, novelty and scope of the study, and outline of the thesis.

Chapter two offers a historical review of nanomaterials used in detection applications, focusing on $Bi_2O_3$, Ag, and Ge nanoparticles, the laser ablation technique for synthesizing these nanoparticles, optimization of synthesis parameters, and the advantages and challenges of this method. Additionally, the chapter reviews the role of ZnO layers in enhancing the stability and performance of nanoparticles, purification techniques, and applications of these nanoparticles in UV photodetectors.

Chapter three describes the methodological approach of this thesis, including the synthesis of $Bi_2O_3$, Ag, and Ge nanoparticles via laser ablation, the fabrication of photodetectors and the characterization techniques employed.

Chapter Four presents the results and discussions of the nanoparticle synthesis, optimization of different parameters as well as the impact of ZnO layer positioning on nanoparticle performance. Additionally, it covers the fabrication and performance of UV photodetectors using the synthesized nanoparticles, including their sensitivity, stability, and efficiency.

Chapter five consists of the conclusions and future works, summarizing the key findings, contributions to the field, and recommendations for further research.

# CHAPTER 2

# LITERATURE REVIEW AND SCIENTIFIC BACKGROUND

## 2.1 Introduction

This chapter is organized into 23 sections and subsections, focusing on the literature review and scientific principles of laser ablation in liquid synthesis methods. It examines the impact of various laser pulse parameters—such as wavelength, pulse duration, repetition rate, fluence/energy density, and the ablation medium—on the morphology and aspect ratio of synthesized nanoparticles (NPs). Additionally, the chapter addresses UV photodetectors and the parameters that influence their performance. Furthermore, it delves into the mechanisms of nanoparticle preparation to enhance ultraviolet photo-detection and concludes with a discussion on the advantages and disadvantages of laser ablation in liquids (LAL).

## 2.2 Introduction of Laser Ablation in Liquids (LAL)

Material ablation through the use of lasers is a prominent technique in laser machining and is widely recognized for its ability to cut, drill, and microstructure under atmospheric conditions, with a particular focus on the surface of the ablated workpiece [33]. The utilization of ultrafast lasers for micro and nano manufacturing is a versatile approach for the advanced materials processing plus serves as the foundation for a burgeoning international field [34, 35]. The incorporation of liquid environments has also garnered attention in laser machining due to its impact on surface quality control [36] and ablation efficiency [37]. The immersion of a workpiece in a liquid or the implementation of a liquid film offers numerous advantages, including the reduction of heat load on the workpiece, the creation of debris-free

treated surfaces [36], the confinement of plasma and vapor, and the enhancement of shock pressure on the surface [38]. As a consequence, laser ablation has long been employed in laser cleaning [39] and laser shock peening [40]. Unlike laser machining, which primarily concentrates on the target surface, LAL is employed for the synthesis of colloids. In this process, the materials subjected to ablation disperse in the liquid, constituting the ultimate product. Unavoidably, a segment of the ablated material experiences chemical oxidation or reduction at the NPs surface in Laser LAL, exemplified by the oxidation of noble metal particle surfaces [18] or NPs that undergo reduction through oxygen vacancies [41]. These imperfections in the produced colloids play a crucial role in creating surface charge and ensuring electrostatic stability. Additionally, defects in volume or surfaces are commonly advantageous for various applications, like optics, catalysis, and energy. Nevertheless, the majority of the colloids generally preserve the identical chemical composition as a bulk targets, encompassing alloys [42], binary [43], and occasionally ternary materials [44]. Therefore, LAL is widely acknowledged as a physiochemical technique that integrates both bottom-up and top-down approaches. The initial processes in this method are controlled by laser plasma and cavitation physics [45, 46]. The laser beam parameters required for LAL typically consist of wavelengths ranging from ultraviolet (UV) [47] (UV) and visible [48] (vis) to near-infrared [49], an average laser fluence of around 0.1−100 J/cm$^2$, and pulse durations from fs [50] to picosecond [51] (ps), nanosecond (ns), [52] microsecond [53] (μs), and millisecond [54] (ms) regimes, extending to continuous-wave (CW) lasers [55]. It should be noted that Continuous Laser Ablation in Liquid (CLAL) currently faces constraints in terms of processing durations in the range of seconds due to the heating of the target, which leads to liquid boiling.

The operational principle of LAL suggests that the most straightforward approach to generating oxide nanoparticles (NPs) involves commencing with a bulk oxide target. Nevertheless, this particular scenario is not frequently encountered in the existing literature. Instead, the majority of studies document the synthesis of oxide NPs through laser ablation in a liquid solution, utilizing a bulk target composed of pure metal. It is important to emphasize that during LAL, the matter released from the solid target inevitably interacts with the molecules present in the liquid solution. This interaction occurs under three distinct conditions, as illustrated in Figure 2.1: 1) at the interface between the ablation plume and the surrounding liquid, 2) within the gas phase inside the cavitation bubble, and 3) within the liquid at ambient temperature and pressure subsequent to the collapse of the cavitation bubble.

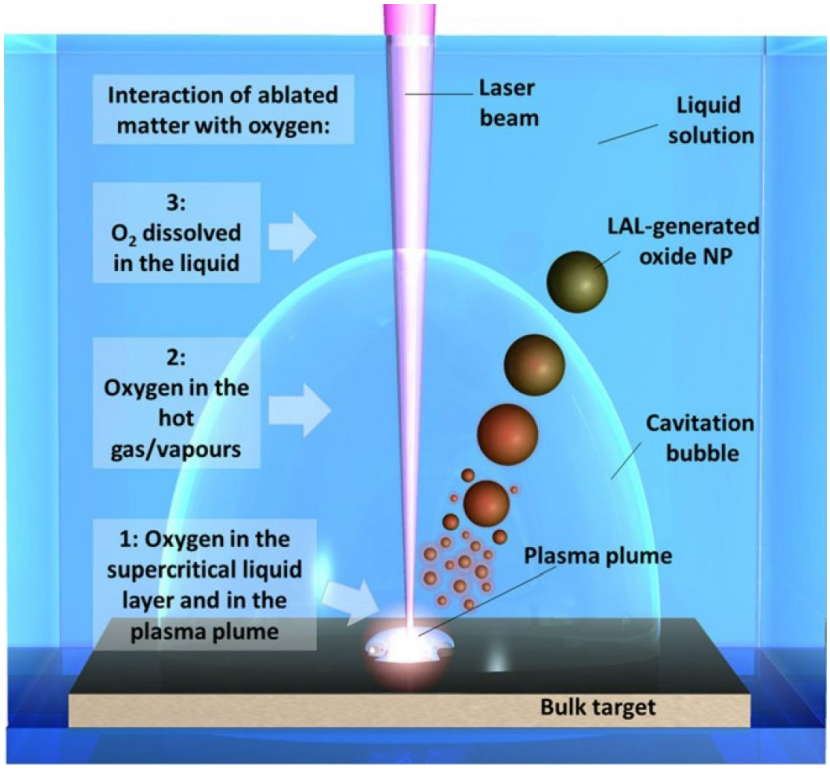


Figure 2.1 Outline of LAL showing target species interactions with oxygen in three zones: within the plasma plume, the cavitation bubble, and the liquid under ambient conditions. AgO microcubes can transition to metallic Ag by modifying LAL parameters, as discussed in [56].

The process known as PLAL can be categorized into three primary stages, as visualized in Figure 2.2. The initial stage, Stage 1, encompasses the interaction between the laser and the liquid medium. This interaction leads to the creation of electron clouds as a result of the absorption of photons by molecules within the liquid medium. Each specific liquid medium will exhibit distinct responses to the laser, resulting in varied outcomes. Stage 2 of the PLAL process involves the laser's interaction with the target. During this stage, the plasma plume is formed, electron clouds participate in the ablation process, cavitation bubbles are generated, and nuclei are formed. Moving on to Stage 3, the growth of nuclei into nanoparticles (NPs) occurs within the cavitation bubble. This growth is facilitated by the involvement of ions from the liquid medium during the nucleation process. Furthermore, the NPs experience collisional events, agglomeration events, and ageing. Numerous physicochemical equations govern the PLAL process, making it challenging to incorporate all of them into a single simulation. Table 2.1 highlights the importance of laser parameters in controlling the size and structure of nanoparticles.

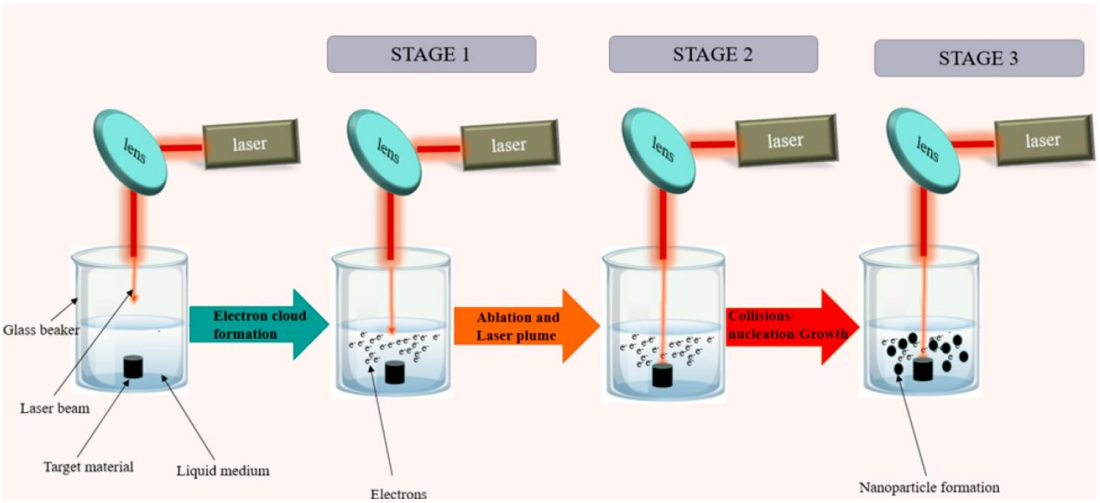


Figure 2.2 The depiction of the PLAL process in batch mode, elucidates the three primary phases of PLAL [57].

Table 2.1 Numerous investigations focusing on diverse metal nanoparticles have elucidated the effects of laser parameters on the modifications of nanoparticle morphology, structure, and properties.

| Studied Metal/Metal Oxide Nanoparticle | Material Role | Laser Parameters | Characteristic Investigated | Application Focus | Reference |
|---|---|---|---|---|---|
| Ag NPs | Plasmonic material, UV absorber | Laser wavelength (355 nm, 532 nm) Laser fluence (38.2, 76.4, 144.6 J/cm$^2$) | Stability and size distribution | Enhanced Ag nanoparticle yield for UV–related optical sensing | [23] |
| Ni NPs | Magnetic material for sensing and catalysis | Laser fluence per pulse (50, 100, 150 mJ) | Structural, optical, antibacterial property | Green synthesis of oxidation-free Ni NPs for magnetic biocatalysis and biosensing | [58] |
| Mg NPs | Metallic component for optoelectronic applications | Laser wavelength (1064 nm) Pulse duration: 7 ns PRR: 10 Hz Ablation time: 10–30 min | Spectral line intensities, plasma parameters | Optoelectronic applications | [25] |
| Ag NPs | Plasmonic | Laser wavelength (800 nm) Pulse width: 40 fs Power 1 mJ PRR: 1 KHz Ablation time: 15 min | Antibacterial efficiency, structural & optical properties | Antibacterial performance in different solvents | [59] |
| CdO NPs | Semiconductor, photocatalyst | Pulse duration: 7 ns Energy per pulse: 80 mJ | Stability, morphology | Photocatalytic and environmental remediation | [60] |

Table 2.1 (Continued)

| Studied Metal/Metal Oxide Nanoparticle | Material Role | Laser Parameters | Characteristic Investigated | Application Focus | Reference |
|---|---|---|---|---|---|
| Au-Ag NPs | Optical limiting nanomaterial | Pulse duration: 7 ns<br>Energy per pulse: 50, 150, 250 mJ | Effect of laser energy on nanostructure | Nonlinear optical limiting for optoelectronic devices | [24] |
| Au NPs | Photocatalyst | Laser wavelength: 1064 nm<br>Pulse width: 8 ns<br>Fluence: 7.28, 17.03, 21.55 and 23.96 J/cm$^2$ | Structural, morphological, optical properties | Photocatalysis, solar cells, biomedical | [61] |
| $TiO_2$ | Visible light photocatalyst | Laser wavelength: 532 nm<br>Pulse width: 10 ns<br>Fluence: 0.65 J/cm$^2$<br>Irradiation time: 45, 60, 75, 90 min | Optical properties, energy bandgap | Visible-light activated photocatalysis | [62] |
| Pd NPs | Catalyst for chemical/electrochemical reactions | Laser wavelength: 1064 nm<br>Pulse width: 10 ns<br>Fluence: 40.5–8 J/cm$^2$<br>Irradiation time: 45, 60, 75, 90 min | Morphology, nanostructure, the effect of fluence on size of nanoparticles | Catalysis and hybrid nanomaterials | [63] |

Table 2.1 (Continued)

| Studied Metal/Metal Oxide Nanoparticle | Material Role | Laser Parameters | Characteristic Investigated | Application Focus | Reference |
|---|---|---|---|---|---|
| Fe based NPs | Co-catalyst for photoelectrodes | Laser wavelength: 1064 nm<br>Pulse width:6 ns<br>PRR: 10 Hz<br>Fluence: 9–21 J/cm$^2$<br>Irradiation time: 2–32 min | Stability, composition | $TiO_2$ photoanode enhancement in water splitting | [64] |
| Cu NPs | Antibacterial and photocatalyst | Laser wavelength: 1064 nm<br>Pulse width: 7 ns<br>PRR: 20 Hz | Structure, morphology, stability, composition | Surface-clean CuOx for catalysis and antibacterial | [65] |
| Al NPs | Heat transfer enhancer | Laser wavelength: 532 nm<br>Ablation time: 15 min<br>PRR: 10 Hz<br>Pulse width: 6 ns | Structure, morphology | Nanofluids for cooling systems | [66] |
| Al NPs | Wide-bandgap semiconductor, UV detector material | Laser wavelength: 1064 nm<br>Ablation time: 15 min<br>PRR: 10 Hz<br>Pulse width: 6–7 ns | Thermal conductivity, optical properties | Optical sensing and UV photodetector applications | [67] |

Table 2.1 (Continued)

| Studied Metal/Metal Oxide Nanoparticle | Material Role | Laser Parameters | Characteristic Investigated | Application Focus | Reference |
|---|---|---|---|---|---|
| $TiO_2$ | Optical and dielectric nanomaterial | Laser wavelength: 532 nm<br>Pulse width: 10 ns<br>Fluence: 0.65 J/cm$^2$<br>Irradiation time: 45, 60, 75, 90 min | Optical properties, energy bandgap | Optical coatings, dielectric layers | [68] |

## 2.3 Influence of laser pulse parameters on the preparation of nanoparticles

### 2.3.1 Impact of laser pulse wavelength

Multiple studies have explored the effect of laser pulse wavelength on the size and shape of laser-ablated nanoparticles (NPs) [69, 70]. Compared to visible wavelengths, both UV and IR wavelengths impact nanoparticle synthesis differently. UV wavelengths, due to their higher photon energy, enhance fragmentation and tend to produce smaller, more uniform nanoparticles. In contrast, IR wavelengths penetrate more deeply into the target, resulting in a higher mass ablation per pulse, which generally yields larger NPs. For metal targets, visible or UV lasers increase the ablation rate due to interband absorption within the UV range, although SPR absorption by the synthesized metal NPs often promotes further fragmentation, leading to smaller NP sizes [71]. This SPR effect can also limit subsequent ablation efficiency by absorbing incident laser energy. Thus, altering laser wavelengths provides a means to control NP size and shape, with shorter wavelengths favoring smaller, more symmetrical NPs and longer wavelengths facilitating larger, potentially varied shapes.

### 2.3.2 Influence of Changes in Laser pulse Duration

The impact of the length of the laser pulse on the laser ablation process has garnered significant attention in the field [42, 72]. Pulse duration determines the time available for energy transfer within the material, and this process is established by how long it takes for electrons in the material to cool down. When using nanosecond pulses, the laser heats the target material, causing it to melt. This molten phase allows atoms to coalesce, typically resulting in larger nanoparticle (NP) sizes with a broader size distribution. In contrast, femtosecond lasers have pulse durations shorter than the electron cooling time, resulting in negligible interaction between electrons and the

lattice. This leads to a 'cold ablation' process where material transitions directly from solid to vapor without significant melting, producing smaller, more uniform NPs [73]. A study comparing the effects of femtosecond, picosecond, and nanosecond lasers in deionized water for NP preparation demonstrated these differences in particle characteristics [72]. Tsuji et al. found that while femtosecond laser pulses produced Ag NPs with a narrower size distribution, they also had lower formation efficiency than those created with nanosecond pulses [73]. Similarly, Barcikowski and co-workers observed that femtosecond pulses resulted in a higher ablation rate than picosecond pulses, supporting the trend toward smaller NP sizes with shorter pulses [74]. Studies have shown that laser pulse duration affects both NP size and shape. Nanosecond pulses, which allow more energy transfer to the material, tend to produce larger, more spherical NPs due to melting and coalescence. In contrast, femtosecond pulses favor the formation of smaller, more uniform NPs due to rapid vaporization, with less influence on NP shape. Therefore, decreasing pulse duration to femtoseconds generally yields smaller NPs with controlled size distributions, while nanosecond pulses can yield larger particles with rounded shapes due to thermal effects.

### 2.3.3 Impact of altering laser pulse width

The pulse duration constitutes a critical parameter in the synthesis of nanoparticles (NPs). Modifying the pulse duration, ranging from nanoseconds (ns) to picoseconds (ps) and femtoseconds (fs), instigates a shift in the ablation mechanism, transitioning from melting and thermal evaporation to phase explosion, respectively. A reduced pulse duration enhances the efficiency of the ablation process, facilitating prompt evaporation and minimizing the heat-affected zone. Particularly in the picosecond range, ablation transpires at an accelerated rate owing to its lower threshold

for metals in comparison to nanoseconds [75]. Additionally, it has been documented that the energy absorbed by the target is relatively low when ultra-short laser pulses are utilized. Thus, employing ultra-short laser pulse durations of picoseconds/femtoseconds offers advantages in terms of enhancing the efficiency of the laser ablation process [76]. The production efficiency remains significantly higher when compared to shorter picoseconds or longer nanoseconds pulsed lasers with similar wavelengths [77].

### 2.3.4 Effect of pulse repetition rate

In general, when considering a specific laser's output, the pulse energy tends to decrease as the repetition rate decreases. This is due to the fact that lower repetition rates result in a higher laser fluence, which in turn leads to an increased yield of ablation at these lower rates. However, there have been reports by Zamiri et al. that demonstrate a contrary trend for laser-ablated Ag nanoparticles when starch is used as a stabilizer [78]. These reports indicate that an increase in particle size was observed with an increase in repetition rate. Similarly, Manjon and co-workers observed a comparable pattern in ablation speed, yet they noted a reduction in particle size with an increase in repetition rate [79]. The decrease in size can be ascribed to the circumstance where the laser pulse duration is shorter than the ablated particles diffusion time. In such cases, the particles undergo multiple irradiations, leading to a reduction in size. Streubel et al. also reported a decrease in ablation yield at higher repetition rates (on the order of MHz) due to a decrease in pulse energy [80]. Pulse repetition rate influences both the size and shape of nanoparticles. Higher repetition rates tend to decrease particle size as repeated irradiations fragment the particles, particularly when diffusion time is longer than the pulse duration. This can lead to

more uniform and potentially smaller particles, while lower repetition rates tend to yield larger particles due to higher energy per pulse. In terms of shape, rapid re-irradiation at high repetition rates can yield spherical or rounded particles due to consistent energy application, whereas lower repetition rates allow more varied, potentially irregular shapes to form as particles are exposed to fewer laser impacts.

### 2.3.5 Effect of fluence/energy density

The onset of the ablation procedure requires a certain threshold energy. When the laser pulse energy is insufficient, the target experiences heating as a result of laser pulse absorption, but this energy is inadequate for ejection from the target and does not give rise to plasma plumes. However, once the threshold is surpassed, the generate of the ablated NPs increases with laser fluence [81, 82]. As the laser fluence continues to rise, the absorption becomes more efficient, thereby enhancing the ablation rate [83]. Additionally, size of ablated NPs decreases with higher laser fluence. The application of a high pump fluence not only triggers the ablation process, but also induces the melting of the target surface, leading to reduced evaporation as well as auto-laser light absorption. Therefore, the absorption-induced fragmentation of larger particles gives rise to the formation of smaller particles [82]. A study by Nikolov and colleagues revealed that NPs size has no impact on laser fluence during ablation at the 1064 nm, whereas it directly affects fluence when NPs are ablated at the 532 nm [84]. Generally, ablation efficiency improves with pulse energy [85]. However, Al-Azawi stated a maximum fluence beyond which ablation effectiveness rapidly declines due to the NPs fragmentation [86].

### 2.3.6 Ablation medium of nanoparticle synthesis

Deionized water, known as DI, is commonly utilized as a liquid medium in laser ablation production of NPs due to its cost-effectiveness, safety, and high heat capacity [87, 88]. This process typically involves the breakdown of water molecules induced by plasma, resulting in the formation of hydroxides or NP oxides. Hydroxyl groups be able to be absorbed on ablated NPs surface, leading to their electrostatic stabilization. Previous studies have explored the impact of water temperature on the ablated NPs size [89-91]. It has been found that ice-cooled water-based laser-ablated NPs tend to have smaller sizes due to faster cooling rate. Conversely, hot water can accelerate the growth rate of ablated NPs and induce the spontaneous growth and self-assembly of colloids into nonspherical morphologies. In a study conducted by A. H. Hamad in 2020, it was observed the ablated NPs size decrease when nanosecond laser pulse was utilized in ice water, in contrast to deionized water at the ambient temperature [89]. Navas and colleagues extensively explored the connection between the size and morphology of synthesized NPs and the temperature of a surrounding solvent [90]. It was observed that laser-ablated ZnO nanoparticles exhibited highly anisotropic growth, transforming from spherical to nanorods, nanoflowers, nanosquares and nanoflakes in the presence of CTAB and ammonia under elevated temperatures.

Furthermore, in 2015, the self-assembly of NPs into nano-networks and nano-chains was reported in an elevated temperature environment [91]. Typically, electric double layer that formed on the ablated NPs surface impedes their growth; however, at higher temperatures, melting of metal NPs led them to fuse and form nanonetworks. Size and morphology of synthesized NPs are influenced by the pH of the ablating medium. Laser ablation of the Zn target in both basic and acidic environments has

been found to generate stable ZnO NPs with the narrow size range [92]. The interaction between OH- and H+ ions with the surface of ZnO helps regulate NPs growth. The ablation of metal NPs in alkaline solutions such as KOH or NaOH, which are effective $CO_2$ absorbers, facilitates the development of amorphous carbon-capped stable metal NPs [93]. Achieving higher stability and reducing the size of NPs is possible by utilizing organic solvents. The organic solvents possess an increased molecular dipole moment, which in turn generates a more robust electric double layer on the ablated NPs surface. Consequently, this leads to an intensified repulsive force between NPs. When it comes to the preparation of NPs by LASIS, the most commonly employed organic solvents are acetone, propanol, ethanol, methanol, and ethylene glycol. The selection of different organic solvents yields different rates of ablation, contingent upon their respective chain length and viscosity [94, 95]. On the other hand, acetone, with its substantial dipole moment, engenders robust double electrical layers on NPs surface, preventing their agglomeration [96]. In comparison to acetone, ethanol exhibits lower polarity, resulting in significant particle instability and heightened aggregation. The decomposition of the organic solvents affected by the absorption of laser energy diminishes the energy employed for ablation, thereby leading to decreased particle productivity. This decomposition process generates air bubbles, which act as hindrances along the laser path. Such an effect is predominantly observed in high-viscosity and low-viscosity solvents, as these are recommended for achieving maximum nanoparticle productivity [97].

## 2.4 Mechanisms of Nanoparticle Synthesis

The application of laser ablation on solid targets in the liquid environment enables the production of nanoparticles with various desirable features, like easily

modifiable surfaces, high purity, unique compositions, and intricate structures, which include doped nanocrystals, nano fluorescents, nano frills, core-shell formations and hollow microspheres [98]. Moreover, laser ablation exhibits various advantageous features including environmental sustainability, a straightforward experimental arrangement without the need of extreme conditions in a controlled environment, and the enduring NPs stability. These nanoparticles are free from any detrimental pollutants or hazardous synthetic reactants [99, 100]. The selection of NPs as case studies is justified due to their significant roles in nanotechnology, particularly due to their catalytic and optical features, as well as the numerous opportunities for chemical stability, surface conjugation, and biocompatibility [101]. Additionally, recently, there is a substantial attention in the laser-assisted NPs synthesis, and these NPs can serve as reference materials of laser ablation. The formation of NPs during the laser ablation process involves various physicochemical reactions, which can be categorized into three distinct mechanisms [42]. Figure 2.3 provides a summary of these three forms of the reaction mechanisms. Mechanism A primarily involves the post-irradiation of the colloidal mixture of the NPs. Mechanism B entails the direct creation of NPs during ablation, while mechanism C involves the absorption of incident laser pulse by the bulk material to generate plasma (C2), subsequently leading to the production of expanded cavitation bubbles. Inside these cavitation bubbles the crystalline nanoparticles (C1) are formed through the processes of coalescence and nucleation.